Proc. Natl. Conf. Theor. Phys. **35** (2010), pp. 235-242

ATOMIC MECHANISM OF HOMOGENEOUS MELTING OF BCC FE AT LIMIT OF SUPERHEATING

TRAN PHUOC DUY, VO VAN HOANG
Department of Physics, Institute of Technology of HochiMinh City, 268 Ly Thuong Kiet Street, District 10, HochiMinh City-Vietnam

Abstract. *Atomic mechanism of homogeneous melting of the bulk body-centered cubic (bcc) Fe has been studied via monitoring spatio-temporal arrangement of liquid-like atoms during heating process. Calculations were performed by molecular dynamics simulation. Liquid-like atoms were detected by the Lindemann criterion of melting. We found that liquid-like atoms occur randomly in crystalline matrix at temperature far below the melting point due to local instability of the crystal lattice. Number of liquid-like atoms increases with increasing temperature and they have a tendency to form clusters and melting occurs when percolated liquid-like cluster is formed in the crystalline model. Occurrence of melting is also accompanied by the sudden changes in various static and thermodynamic quantities. However, total melting can be reached at the point far above the melting one. We found three characteristic temperatures of the homogeneous melting of bcc Fe.*

I. INTRODUCTION

Melting process has been under investigation for decades, however, atomic mechanism of melting is still not well understood. Many theories have been proposed for melting process. Born theory of melting, called mechanical melting, is that when the temperature is high enough, the shear modulus of a perfect crystal vanishes [1]. This theory indicates about the lattice instability leading to melting. In contrast, Lindemann proposed a simpler theory, nearly universal phenomenological criterion, for melting. Lindemanns ratio, melting vibrational displacement fraction of the lattice spacing, should be about a half [2]. After that, Gilvarry revised Lindemann ratio to be about one tenth [3]. Later, Gupta et. al. applied the Lindemanns criterion for monitoring the melting process of face-centered cubic solids [4]. They found that the Lindemann parameter must have one value for all solids which have the same lattice structure, interatomic interaction, but it has different values in case of the same structures with different interatomic interaction. Furthermore, they also proposed the relation between the angular frequencies and the Lindemann parameter. In 1974, via studying the melting process of Argon at high pressure, Ishizaki et. al. confirmed the Lindemanns criterion [5]. The values of the Lindemann ratio for the cubic metals were calculated [6]. Moreover, a universal criterion of melting has been introduced by Lubchenko [7]. This criterion is purely kinematic. They found that the vibrational molecular displacements should be less than the elemental displacements that would occur during the multi-particle structural transitions.

A lot of papers have been written for studying of melting behavior to check the validity of the theories. Manai et al. have used numerical simulations for investigating the melting process of Cu systems in both the bulk and nanometer-sized models [8]. Using

molecular dynamics (MD) simulation, they found that collapse of the crystalline structure is caused by the proliferation of atoms with defective coordination in homogenous melting. Melting of bcc vanadium has been studied via MD simulation [9]. In this paper, author used thick slab model (3 fixed layers at the bottom in z direction, top of it the model is free, periodic boundary conditions for x and y directions). They found that the thermodynamic melting temperature of vanadium is about 2220K at V (111) surface. The surface region of V (111) begins to disorder first at about 1000K [9]. Isobaric-isothermal Monte Carlo simulations have been used for studying melting mechanism of fcc model with Lennard-Jones potential [10]. They concluded that the defects created in the solid phase become numerous enough to cause the crystal melting. The average nearest neighbor numbers decreased with the increasing temperature. Gomez et. al. also confirmed the role of defects in melting mechanism [11]. Delogu et. al. have also used MD simulations for detecting the defects effect on melting [12]. According to their results, heterogeneous and homogeneous melting processes are governed by different mechanisms but all of these processes are caused by defective atoms. In contrast, the homogenous melting of superheated crystals by using MD simulation have also been studied by Forsblom et. al [13]. Their results show that a system with three to four interstitials may eventually return to an ordered lattice, but with six to seven interstitials and three to four vacancies, the system is leaded to melting. Moreover, the melting mechanism of their system is not governed by dislocations, in contrast to [9, 10, 11, 12]. In addition, Ivanov et. al. found a limited contribution of heterogeneous melting under conditions of fast heating [14].

On the other hand, iron was paid a great attention due to its application and being the main earth-core element [15, 16, 17]. Bulk properties of iron in the earth-core conditions were determined by using first principle calculation combined with classical MD [18]. Melting of iron under earth-core conditions has been studied via ab initio calculation [19], or using Monte-Carlo free energy calculation [20]. Experiment on melting of Fe was done by Saxena et. al. [21]. Local icosahedral order in bulk and nano-sized amorphous Fe has been studied in [22, 23] by doing Honeycutt-Andersen (H-A) analysis, using Pak-Doyama potential with MD simulation. However, there is no work related to the studying of atomic mechanism of melting of bcc Fe. Therefore, it motivates us to carry out the MD simulation of homogeneous melting mechanism of bulk bcc Fe via Lindemann criterion of melting. We will discuss in details about atomic mechanism, structural evolution and the effects of defects on the melting.

II. CALCULATIONS

We chose using the Pak-Doyama potential in the present work, i.e it has the form as follows [22]:

$$U(r) = -0.188917(r - 1.82709)^4 + 1.70192(r - 2.50849)^2 - 0.198294(eV), \qquad (1)$$

which has a cut-off radius between the second and third nearest-neighbor distances of α-Fe [22]. This potential described well different structural and mechanical properties of α-Fe and amorphous Fe as well [23]. We builded up the body centered cubic models with 12 unit cells with the length of 2.861 (for α-Fe [24]). Using MD simulation with periodic boundary condition, we relaxed the model for 50,000 MD steps at 50K for getting

equilibrium state at constant zero pressure (i.e. NPT ensemble simulation). Then the models were heating up to the melt. The temperature of the models were increasing linearly by the equation $T = T_0 + \gamma t$ in which $\gamma = 5.26 \times 10^{11} K/s$ is the heating rate, t is the heating time and $T_0 = 50K$ (the initial temperature of the models). We use the Verlet algorithm with MD time step $dt = 0.025\tau_0$, and $\tau_0 = 7.61 \times 10^{-14} s$. So a MD time step is equal to $1.90fs$. Models were heating up until temperature of the system is equal to 2500K . For adapting with statistics, we average the results over two independent runs. We use the cut-off radius $R_0 = 0.264nm$ (corresponding to the minima after the first peak in radial distribution function at 50K), $R_1 = 0.335nm$ (corresponding to the second minima at 50K) for calculating the coordination number.

III. RESULTS AND DISCUSSIONS

III.1. Thermodynamics

Melting points of crystals are the most interesting parameters in studying heating process. From Fig. 1, melting point was identified by defining the sudden increasing of caloric curve. We adopted the melting temperature of bulk bcc Fe in this work as 1915K by selecting the mid-point of the jump on the heating caloric curve like in [25], higher than experimental value of 1811K [24] and lower than the previous simulation result of Evteev et. al. using the same Pak-Doyama potential (i.e it is equal to 2040K). Our melting point is also logically lower than the melting point of Fe under the earth-core condition [19]. Higher value of melting found in the present work is related to the periodic boundary conditions and it is called the superheating. Difference in melting point obtained in the present work compared with the Evteevs one may be related to the difference in number of atoms in models. The energy of fusion can be determined by the variation of the energy at the jump in caloric curve. The energy of fusion of bcc Fe model is found $\Delta E_F = 14.88(kJ/mol)$, which coincides with the experimental value for α-Fe [24] (see Fig. 1).

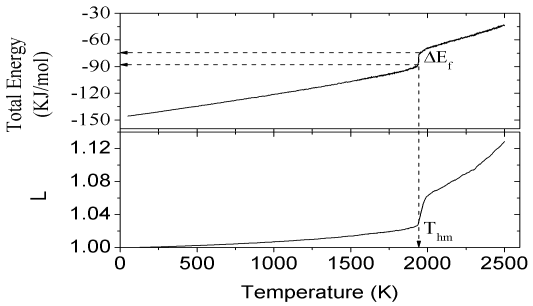

Fig. 1. Caloric curve of melting of bcc-Fe and temperature-dependence of system volume. The arrows with dash lines serve as the guide for eyes

Melting point can be determined by the size parameter, L. The size parameter is calculated as

$$L = \sqrt[3]{\frac{V_T}{V_0}} \tag{2}$$

In (2), V_T is the volume at given temperature and is the volume at initial temperature. The size parameter raises up with increasing temperature due to the loss of compactness of the system. Below melting point, size parameter increases slowly indicating the solid state of the models. In contrast, it has a jump at melting point to enter to the fast increase region of liquid state. In the melting temperature region, we found 3.36% of volume expansion, comparing with 4.3% for 256 atoms of copper bulk systems and 5.1% for 2048 atoms of copper bulk systems in [26].

In addition, one can use the Lindemann criterion for identifying melting point. [27] found that melting at superheating limit was caused by the clusters of destabilized particles inside the bulk crystal. In this paper, we studied the melting process based on Lindemann criterion:

$$\delta_L = \frac{\langle \Delta r^2 \rangle}{\overline{R}} \tag{3}$$

Here, $\langle \Delta r^2 \rangle$ is a root of mean-squared displacement and is a mean interatomic distance taken equal to 2.48 (i.e atomic distance in α-Fe [24]). We determined δ_L via relaxation of model for 5000 MD steps for a given temperature. Note that just 1000 MD steps relaxing is enough for the atoms to escape the a plateau regime of the motion, which is mentioned in [22]. One can find that the Lindemann ratio and density have the same sudden-change at melting point (see Fig. 2). Below the melting point, δ_L increases slightly since it is related to the vibrations of atoms around their positions in solid state. At melting point, due to destroying of crystalline structure, diffusion of atom occurs leading to the sudden change in temperature dependence of δ_L. At $T > T_{HM}$, temperature dependence of δ_L is typical for liquid state. The critical value of Lindemann ratio at melting point was determined, equal to 0.42. In fcc LJ system, it is 0.22 [27], and in bcc crystals is 0.18 [28]. Unlike heterogeneous melting, which is induced by instabilities at the surface, homogeneous melting is basically induced by the defective atoms in the bulk [12]. For this reason, atoms must have large enough rmsd to escape their equilibrium positions and invade the spaces between their neighbours to initiate melting [27]. Because of the nanoparticle surfaces which play the role of the defective region for the melting process to be heterogeneous, the rmsd of the atoms in [29] got to the high enough value at lower temperature than the bulk in this work. Note that the unsaturated bonds of the atoms in the surface made them easily escape the equilibrium positions because of the lower needs of energy to break the bonds. As we use the NPT ensemble, the density of the system is also changed during the melting process. The simulation box is enlarged by the loss of compactment of the system resulting the decreasing of density. Density has inverse behaviors with temperature comparing with other parameters. Note that the initial density of the model is $7.92 g/cm^3$ taken from the experimental value for α-Fe [24].

III.2. Atomic mechanism of melting

In this section, we will discuss about the atomic mechanism of melting. We have found the melting temperature is 1915K in previous section, and determined the critical value of Lindemann ratio $\delta_L = 0.42$. For studying deeply about the mechanism of melting, we calculated the Lindemann particles in the model. The Lindemann particles are the

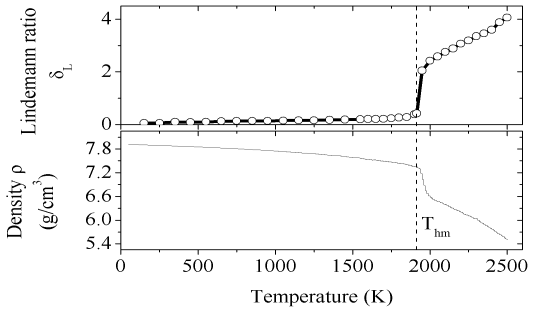

Fig. 2. The variation of Lindemann ratio and system density during the melting process. The vertical dash line is marked for the melting point determined above.

atoms, which are satisfied the condition below

$$\frac{\Delta r^2}{\overline{R}} > \delta_L^* \tag{4}$$

Here, Δr is the root-mean-square displacement of the atoms, $\overline{R}$ is the average nearest neighbor distance and δ_L^* is the critical Lindemann ratio. Atoms, which are not satisfied (4), are considered non-Lindemann particles. We calculated the RDF of Lindemann and non-Lindemann particles during the heating process. In figure 3, the RDFs of Lindemann and non-Lindemann particles are shown together with the total one. We found that RDF of the Lindemann particles exhibits liquid-like behavior while for the non-Lindemann ones, it show solid-like behavior, i.e it has additional peaks of crystalline order. The same results can also be found in [27]. Evolution of fraction of the Lindemann particles on heating is of great interest. That is, the increment of liquid-like atoms is small below the melting point and then it is strongly increase. Fraction of liquid-like atoms $n_{liquid-like}/N$ has a sudden change at melting point (the critical $n_{liquid-like}/N$ is 0.098) and after that it continues increasing to reach maximal value of 1.0 (see Fig. 4). Temperature dependence of fraction of liquid-like atoms on heating is similar to that found for total energy, volume expansion and Lindemann ratio (see Figs. 1, 2 and 4). This indicates their close correlation in the melting process of the system. This can be explained by locally thermal vibration. This scenario is shown clearly in Fig. 5 containing snapshots at the temperature of 1850K, 1900K, 1950K and 2000K. One can see that the liquid-liked atoms appear in such randomly positions. As the results of that, one can conclude that the melt is initialized at random positions in the models at which the local instability is high. When the temperature increases, these liquid-like atoms have significant fraction in the models and seem to form such clusters in the models. Liquid-like atoms occur in the region close to melting one (significant amount of liquid-like atoms was found at around 1800K - 1900K). Fraction of liquid-like atoms increases progressively on further heating and has a tendency to form clusters. The liquid clusters are determined as follows. If the distance between a pair of the Lindemann particles is less than the radius of the first coordination sphere, i.e $R_0 = 2.64$, they belong to the same cluster. In Fig. 4, we also plot the ratio of a size of the largest cluster to the total atoms in the models. We found that liquid-like atoms firstly occur at $T = 1800K$ (this point can be considered as the critical value for

the stability of crystalline structure on heating and denoted as T_{LS}), their number grows up with increasing temperature and they have a tendency to form clusters. Number of liquid-like clusters grows up progressively on further heating and reach a maximal value at homogeneous melting point (T_{hm}) and at the vicinity above this point a percolated liquid-like cluster is forming which spans throughout the model (Fig. 5). This means that homogeneous melting point is related to the percolation threshold of liquid-like clusters. Percolation occurs when total number of liquid-like atoms in the crystalline matrix is large enough, i.e. it reaches a critical value $\rho_C = 0.1$. It is close to the lowest bound of the percolation range proposed for supercooled liquids, i.e. $0.15 < \rho < 0.45$[30]. Furthermore, at the homogeneous melting point, large fraction of atoms is still solid-like and they will melt eventually on further heating to form new additional small liquid-like clusters as found in Fig. 5. Finally, total melting can be reached at around $T_{tm} = 2500K$ (see Figs. 4).

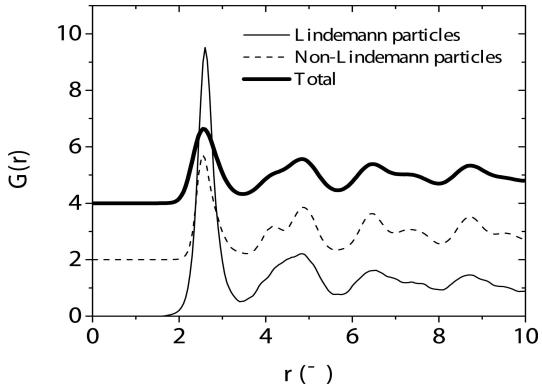

Fig. 3. RDFs of the Lindemann particles, non-Lindemann particles and the total in the models at melting point $T = 1915K$

IV. CONCLUSION

We have studied the melting mechanism of bulk bcc Fe using MD simulation with the Pak-Doyama interatomic potential. The Lindemann criterion is used to analyzed the atomic mechanism of melting. Several conclusions can be made as given below: (i) We found that the melting point of bulk bcc Fe is 1915K. The melting interval is short which characteristic of homogeneous melting. We found temperature dependence of total energy, volume and Lindemann ratio. We found the energy of fusion $\Delta E_F = 14.88(kJ/mol)$. We found the critical Lindemann ratio $\delta_L^* = 0.42$ at the melting point. It is close to that found for bcc metals in practice. (ii) During heating toward melting, we found that mean bond length increases, the coordination number of the first coordination sphere decreases. (iii) We found that the first liquid-like atoms occur randomly in crystalline matrix at $T = 1800K$ (i.e much below the melting point) due to local instability of lattice. Number of liquid-like atoms increases with further heating and they form clusters. In the vicinity of melting point, single percolation liquid-like cluster was formed via merging smaller liquid-like clusters and single liquid-like atoms. Number of liquid-like atoms aggregated into the

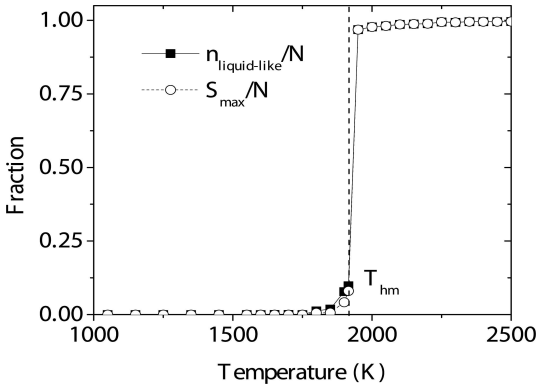

Fig. 4. Fraction of liquid-like atoms in the models ($n_{liquid-like}/N$) and the largest cluster of liquid-like atoms (S_max/N) per total number of atoms in the models during the heating process. The vertical dash line is marked for the melting point determined above

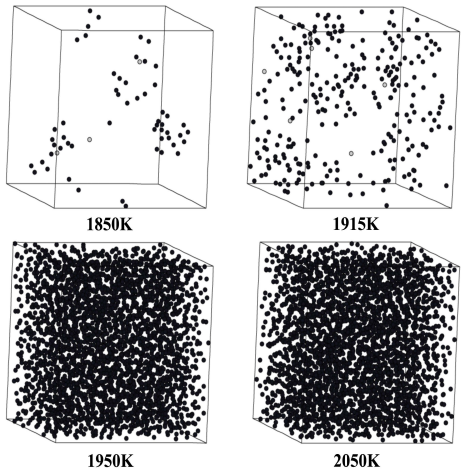

Fig. 5. 3D visualization of the Lindemann particles at different temperature using software written by M. Engel from Stuggart University.

single percolation one progressively grows up to form liquid phase and total melting occurs when their fraction is reaches 1.0. Similar atomic mechanism of homogenous melting on fcc models with LJ potential was found [28].

ACKNOWLEDGMENT

This work was done at the Faculty of Applied Sciences, Institute of Technology, HoChiMinh National University under supervision of Prof. Vo Van Hoang.

REFERENCES

[1] M. Born, K. Huang, *Dynamic Theory of Crystal Lattices*, 1968 Clarendon Press, Oxford.
[2] F. A. Lindemann, *Phys. Z.* **11** (1910) 609.
[3] J. Gilvarry, *J. Phys. Rev.* **102** (1956) 308.
[4] N. P. Gupta, *Sol. Stat. Comm.* **13** (1973) 69; N. P. Gupta, *Int. J. Sol. Structures* **9** (1973) 431.
[5] K. Ishizaki, P. Bolsaitis, I. L. Spain, *Sol. Stat. Comm.* **15** (1974) 1591.
[6] O. P. Gupta, *Materials Science and Engineering* **57** (1983) L3.
[7] V. Lubchenko, *J. Phys. Chem. B* **110** (2006) 18779.
[8] G. Manai, F. Delogu, *Physica B* **392** (2007) 288.
[9] V. Sorkin, E. Polturak, J. Adler, *Phys. Rev. B* **68** (2003) 174103.
[10] L. Gomez, A. Dobry, H. T. Diep, *Phys. Rev. B* **63** (2001) 224103.
[11] L. Gomez, A. Donry, C. Geuting, H. T. Diep, L. Burakovsky, *Phys. Rev. Lett.* **90** (2003) 095701.
[12] F. Delogu, *Phys. Rev. B* **73**(2006) 184108.
[13] M. Forsblom, G. Grimvall, *Phys. Rev. B* **72** (2005) 054107.
[14] D. S. Ivanov, L. V. Zhigilei, *Phys. Rev. Lett.* **98** (2007) 195701.
[15] F. Birch, *J. Geophys. Res* **69** (1964) 4377.
[16] A. E. Ringwood, *Geochem. J.* **11** (1977) 111.
[17] J. P. Poirier, *Phys. Earth Planet. Inter.* **85** (1994) 319.
[18] A. Laio, S. Bernard, G. L. Chiarotti, S. Scandolo, E. Tosatti, *Science* **287** (2000) 1027.
[19] D. Alfe, G. D. Price, M. J. Gillan, *Physical Review B* **65** (2002) 165118.
[20] E. Sola, D. Alfe, *Phys. Rev. Lett.* **103** (2009) 078501.
[21] S. K. Saxena, G. Shen, P. Lazor, *Science* **264** (1994) 405.
[22] V. V. Hoang, *Nanotechnology* **20** (2009) 295703.
[23] V. V. Hoang, N. H. Cuong, *Physica B* **404** (2009) 340.
[24] D. R. Lide (Ed.), *CRC Handbook of Chemistry and Physics*, 1996 CRC Press, New York.
[25] X. Li, J. Huang, *J. Sol. Sta. Chem.* **176** (2003) 234.
[26] T. D. Daff, I. Saadoune, I. Lisiecki, N. H. de Leeuw, *Surface Science* **603** (2009) 445.
[27] Z. H. Jin, P. Gumbsch, K. Lu, E. Ma, *Phys. Rev. Lett.* **87** (2001) 055703.
[28] F. H. Stillinger, *Science* **267** (1995) 1935.
[29] M. Hurley and P. Harrowell, *Phys. Rev. E* **52** (1995) 1694.
[30] M. H. Cohen, G. S. Grest, *Phys. Rev. B* **20** (1979) 1077.

Received 02-10-2010.